



# Honeycomb-like nanocomposite Ti-Ag-N films prepared by pulsed bias arc ion plating on titanium as bipolar plates for unitized regenerative fuel cells

Min Zhang<sup>a,b,\*</sup>, Lin Hu<sup>c</sup>, Guoqiang Lin<sup>c</sup>, Zhigang Shao<sup>a,\*\*</sup>

<sup>a</sup> Fuel Cell R&D Center, Dalian Institute of Chemical Physics, Chinese Academy of Sciences, Dalian 116023, China

<sup>b</sup> School of Physics and Electronic Technology, Liaoning Normal University, Dalian 116029, China

<sup>c</sup> Lab of Materials Modification by Laser, Ion, and Electron Beams, Dalian University of Technology, Dalian 116085, China

## ARTICLE INFO

### Article history:

Received 30 September 2011

Accepted 6 October 2011

Available online 13 October 2011

### Keywords:

Nanocomposite thin film

Ti-Ag-N

Pulsed bias arc ion plating

Bipolar plate

Unitized regenerative fuel cell

## ABSTRACT

Honeycomb-like nanocomposite Ti-Ag-N films are prepared by pulsed bias arc ion plating, and for the first time served as surface modification layer on TA1 titanium as bipolar plates for unitized regenerative fuel cells (URFCs). Phase structure and surface morphology of the coated samples are investigated by XRD and SEM. Corrosion resistance of bare Ti plates and Ti-Ag-N coated samples is evaluated in simulated URFC conditions, and the interface contact resistance (ICR) between bipolar plates and carbon papers is measured before and after potentiostatic polarization tests. Ti<sub>2</sub>N phase with a preferred orientation of (1 1 0) plane is observed in the Ti-Ag-N film. SEM observation indicates that the film appears honeycomb-like and forms a nanocomposite microstructure with Ag nanoparticles embedded in Ti<sub>2</sub>N matrix. Compared to bare titanium plates, the coated sample shows improved corrosion resistance and ultra-low ICR (2 mΩ cm<sup>2</sup> under a compaction pressure of 1.4 MPa). The superior conductivity of the coated sample is attributed to nanocomposite microstructure containing highly conductive Ag nanoparticles, and honeycomb-like rough surface obtained in this study. Nanocomposite Ti-Ag-N coated titanium bipolar plate exhibits prominent interfacial conductivity and excellent corrosion resistance at high potential, being a promising candidate as bipolar plate for applications in URFCs.

© 2011 Elsevier B.V. All rights reserved.

## 1. Introduction

Unitized regenerative fuel cell (URFC) combines polymer electrolyte membrane fuel cell (PEMFC) and polymer electrolyte water electrolyzer into one cell, and can work as both fuel cell and electrolyzer in respective working mode. It is widely considered as promising energy management systems for stationary, transportation and space applications with the merits of high specific energy of more than 400 Wh kg<sup>-1</sup> [1], being free from self-discharge and not being affected by the depth of the discharge or life of the cycle duration [2].

Bipolar plate is one of the most important components in URFCs, which undertakes important functions such as constituting the backbone of stack, conducting currents between cells, facilitating water and thermal management through the stack, and providing

conduits for reactant gases. In order to perform these functions, the bipolar plates should feature excellent corrosion resistance in URFC environments, good electrical conductivity, high mechanical strength, and high capability of gas separation, low cost and easily machining [3].

Bipolar plates (BPPs) for PEMFC have been investigated extensively [4–15], while few reports have been presented on the BPPs for URFCs. The operating environment of URFCs in water electrolysis (WE) mode is much harsher than that in fuel cell (FC) mode. The potential of water electrolysis is usually in the range of 1.4–1.8 V<sub>SCE</sub>, with an atmosphere of O<sub>2</sub> and with pH 2–4. Exposed to such corrosive environments in URFCs, even carbon-based bipolar plates undergo severe corrosion due to the higher potential (>1.4 V<sub>SCE</sub>) in WE mode, resulting in high ICR and poor cell performance. Thus the BPP materials should be highly corrosion resistant.

Titanium is a kind of threshold metal with excellent corrosion resistance [16]. Additionally, titanium plate exhibits the features, like good mechanical strength and weight effectiveness etc. However, titanium tends to be passive in corrosive media, forming an oxide layer which leads to the increase in ICR and decrease in cell performance [17]. Jung et al. [3,18] coated Au and Pt films on titanium as BPPs for URFCs, respectively. They found good performance in single cell experiments but did not report the electrochemical behaviors of the coated samples in detail. What is more, Au and Pt

\* Corresponding author at: School of Physics & Electronic Technology, Liaoning Normal University, No. 850, Huanghe Road Shahekou District, Dalian 116029, China. Tel.: +86 411 84379117; fax: +86 411 84379185.

\*\* Corresponding author at: Fuel Cell R&D Center, Dalian Institute of Chemical Physics, Chinese Academy of Science, Dalian 116023, China. Tel.: +86 411 84379117; fax: +86 411 84379185.

E-mail addresses: [m.zhang@live.com](mailto:m.zhang@live.com) (M. Zhang), [zhgshao@dicp.ac.cn](mailto:zhgshao@dicp.ac.cn) (Z. Shao).

as noble metals are too expensive to be used in URFCs commercially. Thus, surface treatment by cost-effective, good corrosion resistant and highly conductive film is needed. More recently, Zhang et al. [19] coated titanium plates with Ti-Ag films and investigated the performance of the coated plates in simulated URFC environments. The Ti-Ag-coated samples presented good corrosion resistance and conductivity. Meanwhile, the author pointed out that the stability of Ti-Ag/Ti material itself needs further improvement. Therefore, great efforts are still needed to devote to the exploration of advanced materials and microstructure design for the modification layer.

Nanocomposite thin films have been intensely investigated because the combined structures [20–25], which contain two or more components with different physical properties, make it possible to achieve better performance and functionality than do those of each individual component. Selection of matrix and nanoparticle tailors the films with desired properties. However, nanocomposite films are seldom applied in surface modification for BPPs to enhance corrosion resistance and conductivity of metal plates. Thus far, nanocomposite thin films can be synthesized using sol-gel [26], co-sputtering [24], arc ion plating [27,28], or electrodeposition [23] techniques. However, among these methods, arc ion plating is the most cost-effective and efficient deposition process. According to our previous study [11,29,30], arc ion plating, applying a pulsed substrate bias, PBAIP in short, inherits the advantages of arc ion plating, such as high ionized degree, high deposition rate and strong bonding strength, etc. More importantly, a pulsed bias brings new features in this conventional PVD technique, such as reduced droplets, dense films and low-temperature deposition. As a result, films with excellent performance can most likely be obtained. In addition, PBAIP is an environment-friendly process.

In this paper, nanocomposite Ti-Ag-N thin films were employed to improve corrosion resistance and conductivity of Ti plates, and the films were prepared on TA1 titanium bipolar plates by pulsed bias arc ion plating. The corrosion behavior of the Ti-Ag-N coated titanium plates is investigated by electrochemical method in simulated URFC working environments. The ICR is also evaluated before and after potentiostatic polarization tests.

## 2. Material selection and structure design

Excellent conductivity and corrosion resistance are highly desirable for bipolar plates in URFCs. Silver has the highest electrical conductivity of all metals, including copper and gold [31,32]. Titanium nitride is highly anticorrosive, and has good compatibility with Ti plates, which facilitates the film bond tightly to Ti plate. Hereby, Ag and TiN are selected as the components of nanocomposite films. Nevertheless, Ag is prone to be oxidized and then it is no longer highly conductive. The unique microstructure of nanocomposite is designed to solve this problem. Silver is immiscible with TiN or Ti<sub>2</sub>N, hence the films are expected to form a nanocomposite structure with nanoparticles of silver embedded in dense titanium nitride matrix. Surrounded by dense and anticorrosive titanium nitride matrix, Ag particles can exert the function of improving conductivity and keep free from oxidation. Thin Ti-Ag-N film with such a microstructure is expected to combine good corrosion resistance of titanium nitride with high electrical conductivity of Ag particles, which makes it suitable to act as surface modification layer on BPPs.

## 3. Experimental

DSHP-700 arc ion plating system was used in this study to fabricate nanocomposite Ti-Ag-N films. In this system, two opposite targets, Ag and Ti, both 99.9% pure and 55 mm in diameter were mounted at the end of linear ducts that connect to the chamber.

**Table 1**

Composition of TA1 titanium plate used in this study.

Element	TA1 titanium (wt%)
Fe	0.25
C	0.1
N	0.03
H	0.015
O	0.2
Ti	Balance

Stainless steel holders lying in the center of the chamber can rotate and turn simultaneously. The distance between the center of the holder and the targets was 600 mm. A pulsed bias was applied on the holders through the axis.

TA1 titanium was used as the base metal of bipolar plates, and the chemical composition of TA1 was listed in Table 1. The TA1 titanium substrates with size of 100 mm × 100 mm × 0.1 mm were ultrasonically cleaned in ethyl ethanol for 15 min, and then they were polished chemically for 5 min to remove the surface oxide layer. After washed with deionized water several times, they were blown dry and put on holders. The chamber was evacuated to a base pressure below  $5.0 \times 10^{-3}$  Pa using a turbo molecular pump and a rotary pump. Prior to the deposition, the substrates were sputtered by Ar ions for 10 min with a pulsed bias of –800 V in ambient Ar at 2.0 Pa.

When the deposition began, the working pressure was adjusted to and kept at 0.5 Pa, and the bias voltage, frequency and duty cycle of the pulsed bias were –300 V, 20 kHz and 40%, respectively. Ti target was first burnt to deposit a Ti interlayer to enhance the bonding property. 10 min later, nitrogen gas was introduced in the chamber and the flow rate was 40 sccm, Ag target was burnt simultaneously. Arc current of Ti and Ag targets was kept constant at 80 and 60 A respectively. The thickness of Ti-Ag-N films was controlled to 1.5 μm by adjusting deposition time.

Phase structure was detected with XRD-6000 X-ray diffractor. Surface morphology was observed with scanning electron microscopy (JSM-5600LV) equipped with energy dispersive X-ray spectroscopy (EDX). The ICR between uncoated, coated bipolar plates and diffusion layer (carbon paper) was measured with the conventional method extensively used by many researchers [9,14,33,34]. In the set up, two pieces of Toray carbon paper were sandwiched between the bipolar plate sample and two copper plates. The copper plates were plated with gold on both sides to enhance conductivity. An electrical current of 5.0 A, sourced by a PSP-2010 programmable power supply, was provided via the two

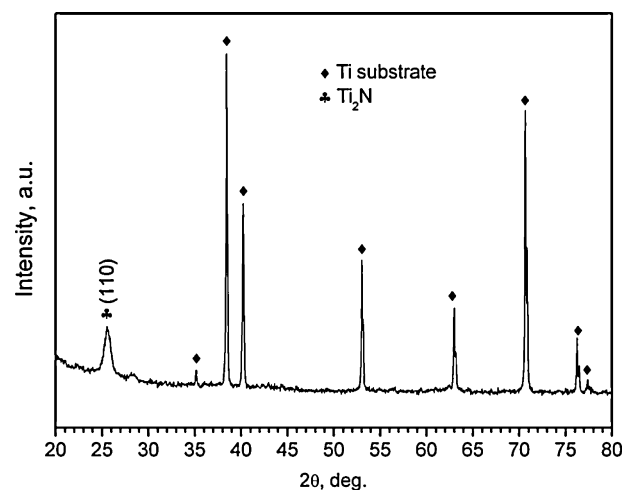


**Fig. 1.** XRD pattern of Ti-Ag-N coated Ti plate.

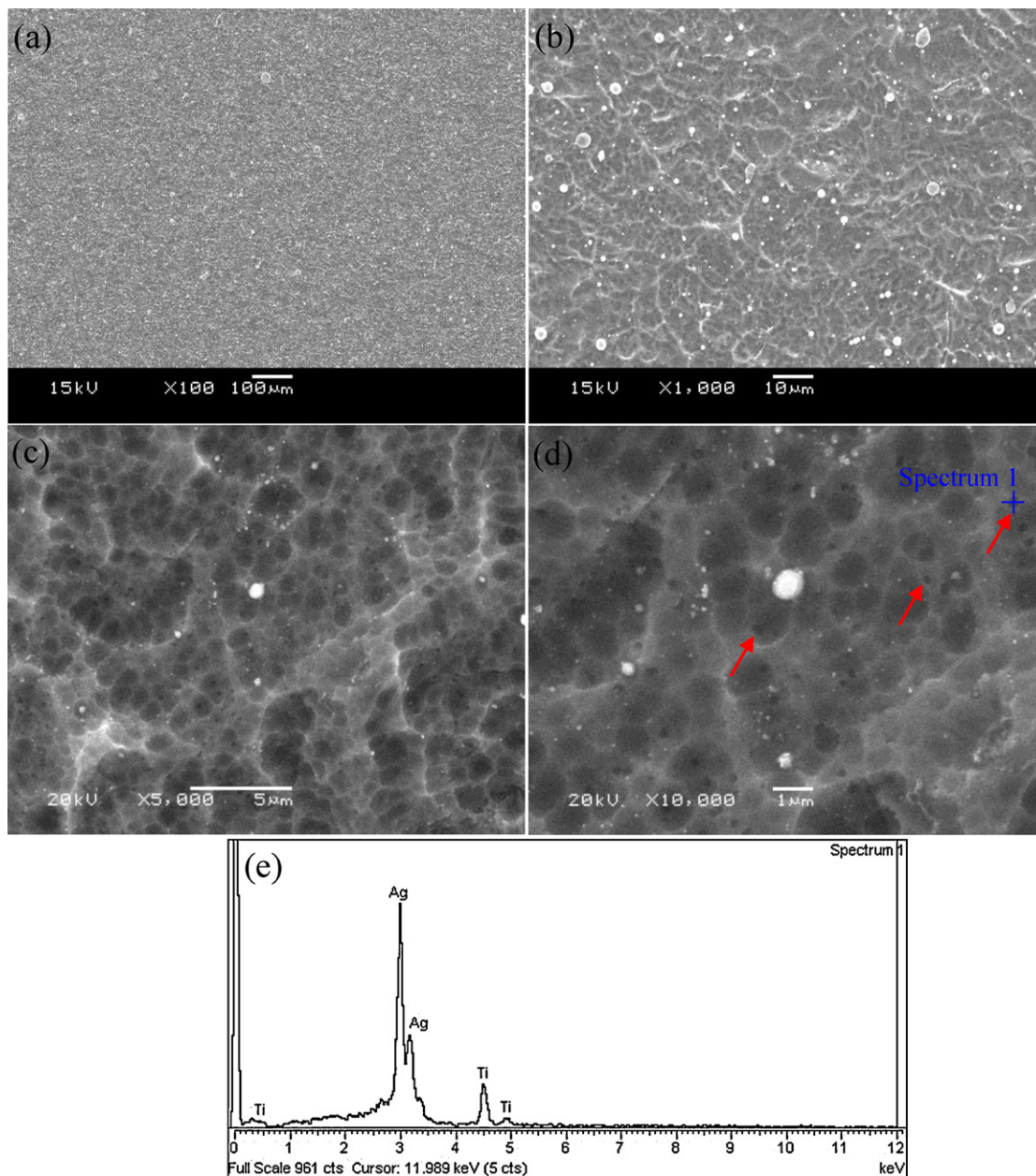


Fig. 2. SEM images of nanocomposite Ti-Ag-N films: (a) 100 $\times$ , (b) 1000 $\times$ , (c) 5000 $\times$ , (d) 10,000 $\times$ , and (e) EDX spectrum.

Au-plated copper plates. During the tests, the compacting force was increased gradually at a step of  $5 \text{ N s}^{-1}$  controlled by a universal WDW electromechanical machine.

Corrosion resistance of the bare and coated Ti plates was investigated by polarization electrochemical experiments using a potentiostat Model 2273A by EG&G Princeton Applied Research and analyzed with the corrosion software of EG&G Version 2.43.0. To simulate an aggressive URFC environment, a  $0.5 \text{ M H}_2\text{SO}_4 + 2 \text{ ppm F}^-$  solution at  $70^\circ\text{C}$  was used, bubbled with either hydrogen gas (simulating a URFC hydrogen electrode environment) or pressured air (simulating the oxygen electrode environment) throughout the electrochemical tests. A conventional three-electrode system was used in the electrochemical measurements, in which a platinum sheet acted as the counter electrode, a saturated calomel electrode (SCE, saturated KCl) as the reference electrode and the stainless steel sample as the working electrode. The size of the working electrodes was  $15 \text{ mm} \times 15 \text{ mm} \times 0.1 \text{ mm}$ . The edges were sealed by insulating epoxy resin, only leaving

a  $10 \text{ mm} \times 10 \text{ mm}$  surface exposed to the electrolyte. As for the potentiodynamic polarizations, the samples were stabilized at open circuit potential (OCP) for 10 min, and then the potential was swept from the OCP in the anodic direction at a scanning rate of  $20 \text{ mV s}^{-1}$ .

In order to evaluate the long-term stability of the samples in the actual working conditions of URFCs, potentiostatic polarizations were performed for over 6.5 h. During the measurements, the specimens were also stabilized at open circuit for 10 min. The current density as a function of time were recorded at hydrogen electrode ( $-0.1 \text{ V}_{\text{SCE}}$ ) and oxygen electrode ( $+2.0 \text{ V}_{\text{SCE}}$ ) potentials for URFCs.

## 4. Results

### 4.1. Phase structure

XRD pattern of the Ti-Ag-N coated Ti plate is shown in Fig. 1. Apart from the diffraction peaks from titanium substrates, only

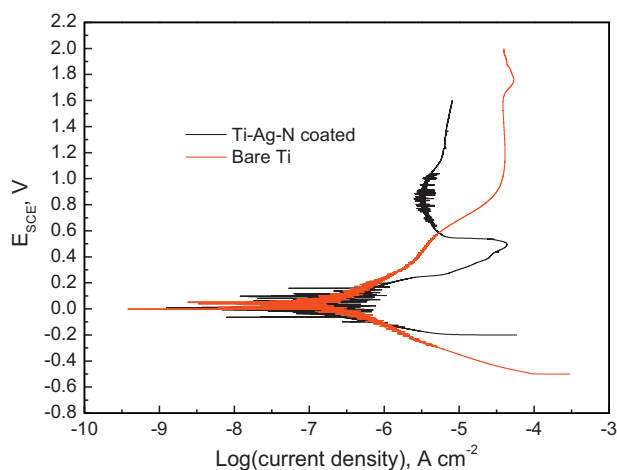


**Fig. 3.** Potentiodynamic polarization curves of the uncoated and coated samples in 0.5 M H<sub>2</sub>SO<sub>4</sub> with 2 ppm F<sup>-</sup> solution at room temperature.

the diffraction peak by the plane of Ti<sub>2</sub>N (1 1 0) are observed. It can be concluded that the film mainly consists of Ti<sub>2</sub>N phase. No diffraction peaks of Ag or related compounds were found in the pattern, indicating that Ag might exist in the form of separated nanoparticles.

#### 4.2. Surface morphology

To analyze the film clearly from macroscopic down to micro-cosmic scales, SEM images of the Ti-Ag-N film with different magnitudes of enlargement are shown in Fig. 2. From Fig. 2a and b, it can be seen that Ti-Ag-N film is coated homogeneously and uniformly on the Ti plates, and there are some Ti or Ag droplets on film surface, which is an inherent feature of arc ion plating process. With an enlargement of 5000× and 10,000×, as shown in Fig. 2c and d, we can see that the film appears honeycomb-like (Fig. 2c), some nanoparticles with a size of 100–200 nm, as pointed out by red arrows in Fig. 2d, are evenly distributed and embedded in titanium nitride matrix. It is the typical microstructure of nanocomposite materials.

To identify the composition of the nanoparticles, composition analysis by EDX point scanning is performed at the blue cross-mark in Fig. 2d, and Fig. 2e presents the EDX data. The main ingredient is Ag, and the minor signal of Ti derives from the error caused by electron beam drifting. Thus, the nanoparticles are proved to be silver particles.

#### 4.3. Corrosion tests

The potentiodynamic polarization of the bare Ti plate and Ti-Ag-N coated Ti plate in 0.5 M H<sub>2</sub>SO<sub>4</sub> with 2 ppm F<sup>-</sup> solution is performed at room temperature, as shown in Fig. 3, to tentatively evaluate the improvement of corrosion resistance by the surface modification proposed in this work. Corrosion current determined by Tafel method and corrosion potential of the coated sample are almost the same with that of the bare Ti. But passive current density decreases from 10<sup>-4.2</sup> A cm<sup>-2</sup> for the bare Ti to 10<sup>-5</sup> A cm<sup>-2</sup> for Ti-Ag-N coated samples, indicating better long-term stability of the coated samples in URFC corrosive media. It is worthy to note that in case of Ti-Ag-N coated samples, a transition region occurs between activation and passivation processes. We think it is attributed to an oxidation process, which always acts as the beginning of passivation process and prevents the corrosion going on. In this work, the oxidation may occur within chemically active areas, for instance, N-poor and Ti-rich film surface containing much departing Ti, around

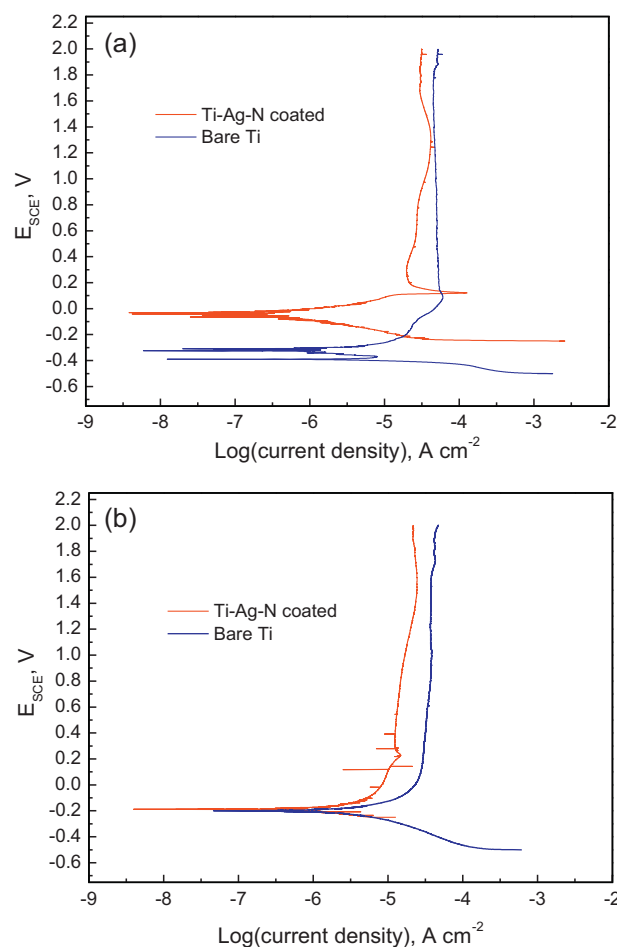


**Fig. 4.** Potentiodynamic polarization curves of the uncoated and coated samples in 0.5 M H<sub>2</sub>SO<sub>4</sub> + 2 ppm F<sup>-</sup> solution at 70 °C with (a) air and (b) H<sub>2</sub> bubbling.

Ti or Ag macro-particles. The transition region does not occur in case of bare Ti plates, because a dense oxide film already forms on Ti plate surface before corrosion tests.

To simulate close enough to the actual URFC working environment, test solution, in which polarizations are performed, is heated to and kept at 70 °C, and is purged with air or H<sub>2</sub> bubbling throughout the electrochemical tests. Potentiodynamic polarization curves of the uncoated and coated samples are shown in Fig. 4. It is obvious in Fig. 4a that after coated with Ti-Ag-N, corrosion potential of the sample gets higher, corrosion current becomes lower, and passive current density keeps much lower. It can be concluded that the Ti plates coated with nanocomposite Ti-Ag-N film exhibit better corrosion resistance and stability than the bare Ti plates. For the hydrogen electrode side, as shown in Fig. 4b, corrosion potential and current of the coated and uncoated samples are almost the same, but passive current density of the coated sample keeps much lower than that of bare Ti plate, showing better corrosion resistance and stability.

To investigate the long-term stability of Ti-Ag-N coated Ti plates, potentiostatic polarization is carried out over 6.5 h in 0.5 M H<sub>2</sub>SO<sub>4</sub> + 2 ppm F<sup>-</sup> solution at 70 °C to simulate the environment of URFCs in WE mode. The results of potentiostatic polarization measurements for Ti-Ag-N coated Ti plates in simulating O<sub>2</sub> and H<sub>2</sub> electrode environments of URFCs are respectively shown in Fig. 5a and b. In both simulated URFC environments, the transient current density decays quite fast in the early stage, then gradually decreases, and lastly stays at a very low level. This implies that as soon as the whole surface is covered by the passive film, the

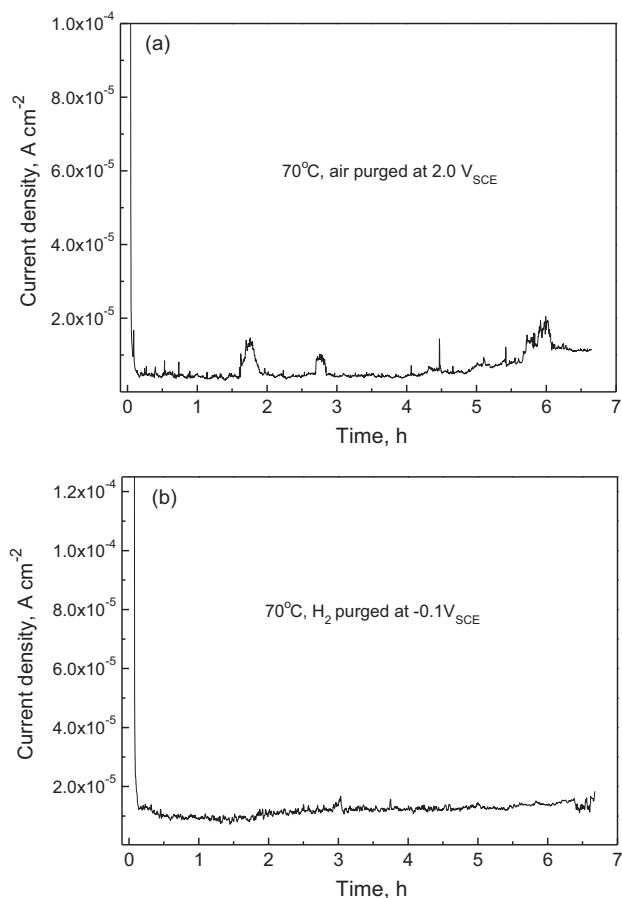


Fig. 5. Potentiodynamic polarization curves of the uncoated and coated samples in 0.5 M  $\text{H}_2\text{SO}_4 + 2 \text{ ppm F}^-$  solution at 70 °C with (a) air and (b)  $\text{H}_2$  bubbling.

current density which is necessary to maintain the passivation becomes rather low. The fluctuation of transient current density may be results from the scattered Ti or Ag macroparticles on the film surface, as shown in Fig. 2b. The current density of both electrodes keep stables around  $1.0 \times 10^{-5} \text{ A cm}^{-2}$  in the last stage, suggesting a good stability of the coated sample.

Fig. 6 presents surface morphology of Ti-Ag-N coated samples before and after 6.5-h potentiostatic polarization tests. Fig. 6a shows the surface morphology of the as-deposited Ti-Ag-N films on Ti plates. The film is dense, homogeneous with scattered solidified droplets, and tightly adhesive to the substrate. After 6.5-h potentiostatic polarization, the film still keeps good integrity and no peeling off or flaking off is observed throughout the testing areas, as shown in Fig. 6b and c. Droplets become fewer owing to preferred dissolution into acid solutions by gas bubbling, resulting in the formation of some pits or micro-cracks (see black arrows in Fig. 6c) on the surface of the samples after air-purged potentiostatic polarization. It implies that the aggressive extent of corrosion in simulated air-purged environment is severer than that in simulated  $\text{H}_2$ -purged environment, which is consistent with the results of corrosion testing (Fig. 5a).

To summarize, Ti-Ag-N coated Ti plates exhibit better stability and corrosion resistance in simulated URFC environments than the bare Ti plates.

#### 4.4. ICR measurements

Fig. 6 shows the ICRs of the bare and Ti-Ag-N coated Ti plates, as the black and red lines indicate. After Ti-Ag-N coated, ICRs of the Ti plate decrease greatly, from 55.2 to 2.3  $\text{m}\Omega \text{ cm}^{-2}$  at the compaction

pressure of  $140 \text{ N cm}^{-2}$ , comparable with the values obtained for Ag-coated Ti plates [19], implying the conductivity of the sample has been improved significantly by surface modification with nanocomposite Ti-Ag-N films.

Maintaining good conductivity of bipolar plates after passivation process is essential for URFC to obtain high power output and long-term stability. Measuring the ICRs between bipolar plates and diffusion layer (carbon paper) after potentiostatic polarization over 6.5 h is necessary and valuable for evaluating the stability of Ti-Ag-N coated samples. The ICRs of the coated samples after potentiostatic polarization over 6.5 h in simulating  $\text{H}_2$  and  $\text{O}_2$  electrode environments are plotted in Fig. 6, as the blue and green line indicates respectively. After potentiostatic polarization over 6.5 h in simulating either  $\text{H}_2$  or  $\text{O}_2$  electrode environment, the ICR of Ti-Ag-N coated sample increases slightly, from 2.3 to around 7  $\text{m}\Omega \text{ cm}^{-2}$  under  $140 \text{ N cm}^{-2}$  compaction pressure.

According to the ICR results, it can be inferred that the conductivity of Ti plates is significantly improved by coating nanocomposite Ti-Ag-N film, even in harsher condition of URFCs in WE working mode.

## 5. Discussion

As bipolar plates in URFCs, the main challenge of Ti plates is to keep good conductivity. Ti plate always presents good corrosion resistance by passivation process in URFC highly corrosive media. As a result, a dense oxide film with poor conductivity forms on Ti plate surface, which leads to a large increase in ICR and decline in cell performance. Additionally, the passivation process will lead to a release of metal ions, such as Fe and Ti ions etc., which can contaminate the electrolyte membrane and poison the electrode catalysts.

In this work, nanocomposite Ti-Ag-N film is applied as surface modification layer to improve conductivity and corrosion resistance of Ti plates. Silver is immiscible with TiN or  $\text{Ti}_2\text{N}$ , so the film will form a nanocomposite microstructure with Ag nanoparticles embedded in titanium nitride matrix. The nanocomposite film is expected to combine high conductivity of Ag with good corrosion resistance of titanium nitride.

The results obtained in this study reveal that after coated with nanocomposite Ti-Ag-N films, Ti plate presents superior corrosion resistance, even at high potential of  $2.0 \text{ V}_{\text{SCE}}$  and in high oxidation atmosphere, as shown in Figs. 4a and 5a. More importantly, after coated with nanocomposite Ti-Ag-N films, the conductivity of Ti plates is significantly improved, even better than that of Ag-coated Ti plates [19], the ICR only 2  $\text{m}\Omega \text{ cm}^{-2}$  under  $140 \text{ N cm}^{-2}$  compaction pressure. After potentiostatic polarization over 6.5 h, the ICR increases slightly, as shown in Fig. 6 (Fig. 7).

The improvements of conductivity by coating nanocomposite Ti-Ag-N thin films are attributed to two aspects. The first is the synergistic function of nanocomposite microstructure and high conductivity of Ag nanoparticles. The microstructure of the films obtained in this study is nanocomposite with Ag nanoparticles embedded in titanium nitride matrix, as shown in Fig. 2d. Titanium nitride is highly conductive ceramic, in which electrons can easily transfer along certain paths. Ag nanoparticles are evenly embedded in the matrix, and act as relay stations for electrons, making electrons transfer much easier with less resistance. Resultantly, the transmitting efficiency of electrons is highly enhanced. The second is the rough surface like honeycomb. Since the gas diffusion layer, i.e. carbon paper, is soft, the pits of honeycomb-like rough surface will be fully filled with carbon fiber under a certain compaction pressure. The effective contact area between carbon paper and the coated Ti plate increases significantly, with point contact changing to surface contact. As a result of these aspects, the conductivity

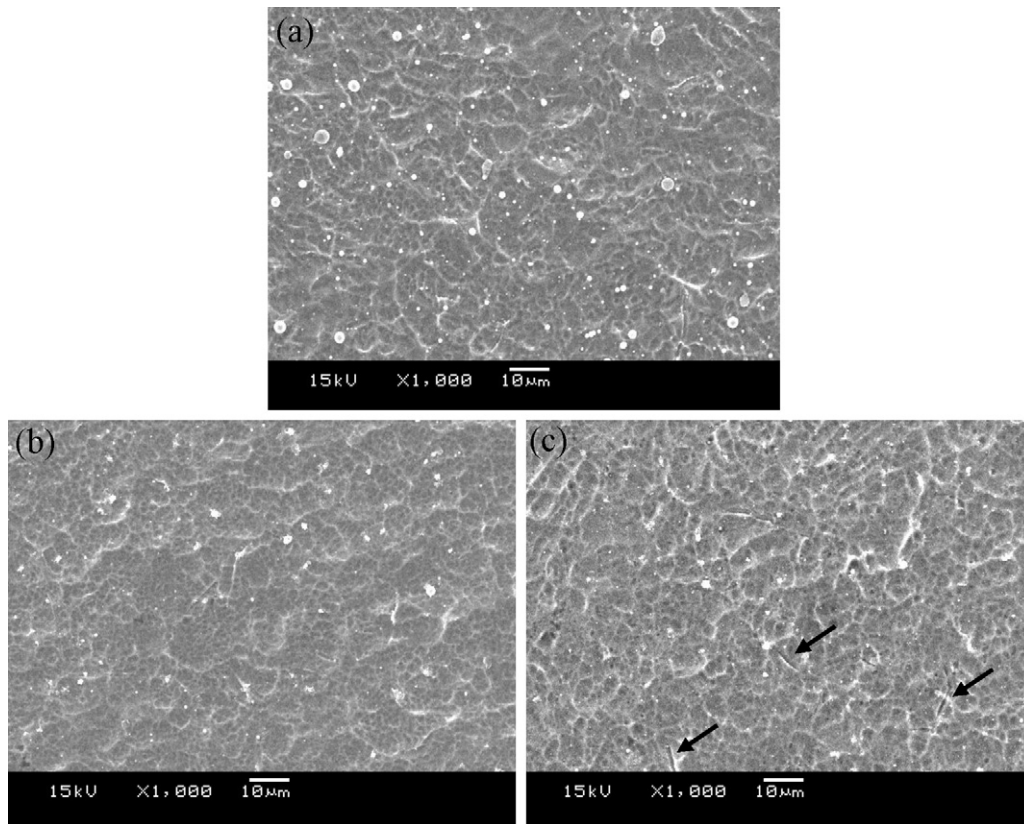


**Fig. 6.** Surface morphology of Ti-Ag-N coated Ti plates before (a) and after potentiostatic polarization test for over 6.5 h in simulated solution at 70 °C bubbled with H<sub>2</sub> at  $-0.1 V_{SCE}$  (b) and with air at  $2.0 V_{SCE}$  (c).

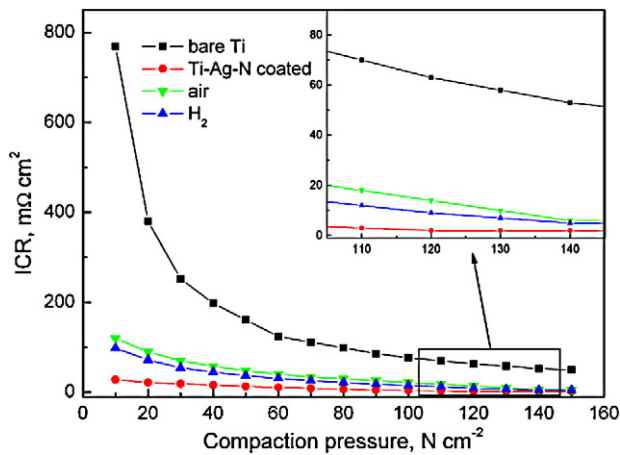


**Fig. 7.** ICRs of the bare and Ti-Ag-N coated Ti plates, and of the coated samples after potentiostatic polarization test in 0.5 M H<sub>2</sub>SO<sub>4</sub> + 2 ppm F<sup>-</sup> solution at 70 °C bubbled with air at  $2.0 V_{SCE}$  (▼) and with H<sub>2</sub> at  $-0.1 V_{SCE}$  (▲) for over 6.5 h.

of Ti plates is greatly enhanced by coating such a honeycomb-like nanocomposite Ti-Ag-N thin films.

## 6. Conclusions

Nanocomposite Ti-Ag-N thin films are applied in this work and deposited by pulsed bias arc ion plating to improve corrosion resistance and conductivity of Ti bipolar plates used in URFCs. The film exhibits a honeycomb-like morphology and exists in a nanocomposite microstructure with Ag nanoparticles evenly embedded in dense Ti<sub>2</sub>N matrix. After coated nanocomposite Ti-Ag-N films, Ti

plate shows superior corrosion resistance and excellent conductivity. The superior conductivity of the coated sample is attributed to nanocomposite microstructure containing highly conductive Ag nanoparticles, and honeycomb-like rough surface obtained in this study. Nanocomposite Ti-Ag-N coated titanium plate exhibits prominent interfacial conductivity and excellent corrosion resistance at high potential, being a promising candidate as bipolar plate for applications in URFCs.

## Acknowledgements

This work was financially supported by the China Postdoctoral Science Foundation (Grant No. 20110491545) and the National Natural Science Foundations of China (Grant Nos. 20936008 and 21076208).

## References

- [1] F. Mitlitsky, B. Myers, A.H. Weisberg, *Energy & Fuels* 12 (1998) 56–71.
- [2] W. Smith, *Journal of Power Sources* 86 (2000) 74–83.
- [3] H.-Y. Jung, S.-Y. Huang, P. Ganesan, B.N. Popov, *Journal of Power Sources* 194 (2009) 972–975.
- [4] L. Wang, D.O. Northwood, X. Nie, J. Housden, E. Spain, A. Leyland, A. Matthews, *Journal of Power Sources* 195 (2010) 3814–3821.
- [5] M.P. Brady, H. Wang, J.A. Turner, H.M. Meyer III, K.L. More, P.F. Tortorelli, B.D. McCarthy, *Journal of Power Sources* 195 (2010) 5610–5618.
- [6] C.-Y. Bai, T.-M. Wen, M.-S. Huang, K.-H. Hou, M.-D. Ger, S.-J. Lee, *Journal of Power Sources* 195 (2010) 5686–5691.
- [7] B. Wu, Y. Fu, J. Xu, G. Lin, M. Hou, *Journal of Power Sources* 194 (2009) 976–980.
- [8] J. Liu, F. Chen, Y. Chen, D. Zhang, *Journal of Power Sources* 187 (2009) 500–504.
- [9] H.S. Choi, D.H. Han, W.H. Hong, J.J. Lee, *Journal of Power Sources* 189 (2009) 966–971.
- [10] A. Pozio, F. Zaza, A. Masci, R. Silva, *Journal of Power Sources* 179 (2008) 631–639.
- [11] Y. Fu, M. Hou, G. Lin, J. Hou, Z. Shao, B. Yi, *Journal of Power Sources* 176 (2008) 282–286.
- [12] J. Barranco, F. Barreras, A. Lozano, M. Maza, *Journal of Power Sources* 196 (2011) 4283–4289.

- [13] H. Wang, J.A. Turner, *Fuel Cells* 10 (2010) 510–519.
- [14] S.B. Lee, K.H. Cho, W.G. Lee, H. Jang, *Journal of Power Sources* 187 (2009) 318–323.
- [15] M. Zhang, B. Wu, G. Lin, Z. Shao, M. Hou, B. Yi, *Journal of Power Sources* 196 (2011) 3249–3254.
- [16] U. Wittstadt, E. Wagner, T. Jungmann, *Journal of Power Sources* 145 (2005) 555–562.
- [17] S.S. Dibrab, K. Sopian, M.A. Alghoul, M.Y. Sulaiman, *Renewable Sustainable Energy Reviews* 13 (2009) 1663–1668.
- [18] H.-Y. Jung, S.-Y. Huang, B.N. Popov, *Journal of Power Sources* 195 (2010) 1950–1956.
- [19] H. Zhang, M. Hou, G. Lin, Z. Han, Y. Fu, S. Sun, Z. Shao, B. Yi, *International Journal of Hydrogen Energy* 36 (2011) 5695–5701.
- [20] S. Tan, X. Zhang, X. Wu, F. Fang, J. Jiang, *Journal of Alloys and Compounds* 509 (2011) 789–793.
- [21] C. Tseng, J. Hsieh, W. Wu, S. Chang, C. Chang, *Thin Solid Films* 516 (2008) 5424–5429.
- [22] P.R. Willmott, J.R. Huber, *Reviews of Modern Physics* 72 (2000) 315–323.
- [23] Guang-Ren Shen, Cheng Yu-Ting, L.-N. Tsai, *IEEE Transactions on Nanotechnology* 4 (2005) 539–547.
- [24] C.P. Mulligan, T.A. Blanchet, D. Gall, *Surface and Coatings Technology* 204 (2010) 1388–1394.
- [25] S. Zhang, N. Ali, *Nanocomposite Thin Films and Coatings: Processing, Properties and Performance*, Imperial College Press, London, 2007.
- [26] Ming Liu, Xin Li, Jing Lou, Shijian Zheng, Kui Du, N.X. Sun, *Journal of Applied Physics* 102 (2007), 083911–083911–083913.
- [27] H.Y. Lee, K.H. Nam, J.S. Yoon, J.G. Han, Y.H. Jun, *Surface and Coatings Technology* 146–147 (2001) 532–536.
- [28] H.S. Lee, D.B. Lee, *Materials Science Forum* 569 (2008) 57–60.
- [29] M. Zhang, G. Lin, C. Dong, L. Wen, *Surface and Coatings Technology* 201 (2007) 7252–7258.
- [30] M.D. Huang, Y.P. Lee, C. Dong, G.Q. Lin, C. Sun, L.S. Wen, *Journal of Vacuum Science & Technology A-Vacuum Surfaces and Films* 22 (2004) 250–256.
- [31] [http://en.wikipedia.org/wiki/Electrical\\_resistivity\\_and\\_conductivity](http://en.wikipedia.org/wiki/Electrical_resistivity_and_conductivity).
- [32] <http://en.wikipedia.org/wiki/Silver>.
- [33] H. Wang, M.A. Sweikart, J.A. Turner, *Journal of Power Sources* 115 (2003) 243–251.
- [34] W. Yoon, X. Huang, P. Fazzino, K.L. Reifsnider, M.A. Akkaoui, *Journal of Power Sources* 179 (2008) 265–273.